Supporting Information

C_2H_2 capture and separation in a MOF based on Ni_6 trigonal-prismatic units

Bin Zhang,[a] Xiu-Yuan Li,[b] Yu-Ke Lu,[a] Lei Hou,*[a] Yao-Yu Wang[a] and Zhonghua Zhu[c]

[a]Key Laboratory of Synthetic and Natural Functional Molecule of the Ministry of Education, Shaanxi Key Laboratory of Physico-Inorganic Chemistry, College of Chemistry & Materials Science, Northwest University, Xi'an 710069, P. R. China. *Email: lhou2009@nwu.edu.cn

[b]Shaanxi Key Laboratory of Optoelectronic Functional Materials and Devices, School of Materials Science and Chemical Engineering, Xi'an Technological University, Xi'an 710032, P. R. China

[c]School of Chemical Engineering, The University of Queensland, Brisbane, 4072, Australia

Materials and general methods.

All solvents were purchased commercially. Elemental analyses of C, H, and N were determined with a Perkin-Elmer 2400C elemental analyzer. Powder X-ray diffraction (PXRD) data were recorded on a Bruker D8 ADVANCE X-ray powder diffractometer (Cu Kα, λ = 1.5418 Å). Thermalgravimetric analyses (TGA) were carried out in a nitrogen stream using a Netzsch TG209F3 equipment at a heating rate of 10 °C min^{-1}. Single crystal diffraction data were collected on a Bruker SMART APEX II CCD single crystal diffractometer (Supporting Information). Adsorption measurements were performed with an automatic volumetric sorption apparatus (Micrometrics ASAP 2020M and TriStar II 3020).

Synthesis of NH_2-H_4BPTC.

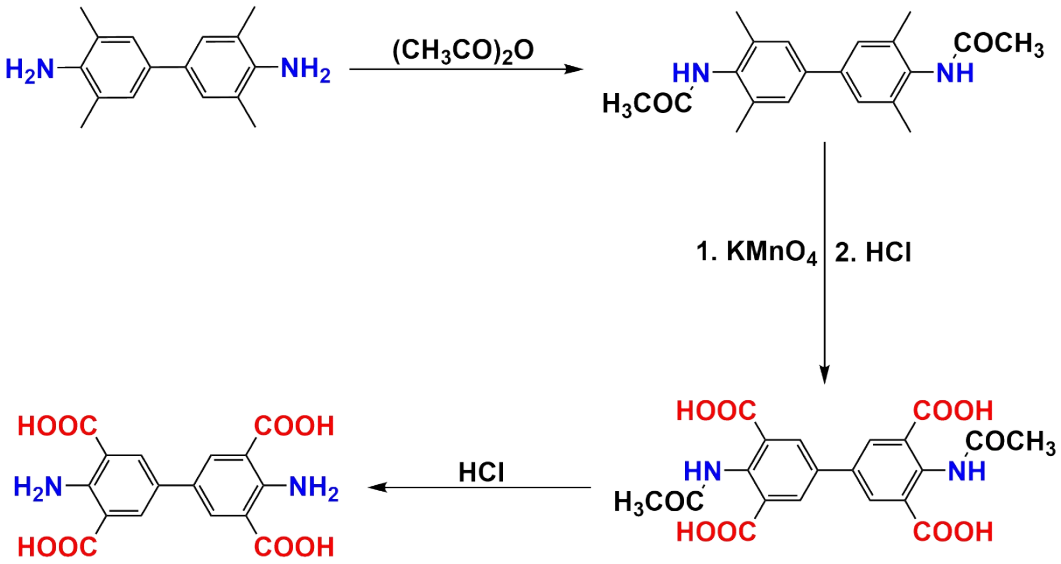

Scheme S1: Representation of the synthetic protocol followed for the synthesis of NH_2-H_4BPTC.

Step 1: 3.6 g of 3,3',5,5'-tetramethyl-[1,1'-biphenyl]-4,4'-diamine, 2.6 mL of triethylamine and 2.9 mL of acetic anhydride are added into 20 mL dichloromethane, and the resulting solution is stirred for 3 hours at room temperature. The white precipitate is filtered, washed copiously with deionized water, and dried at 70 °C to give N,N'-(3,3',5,5'-tetramethyl-[1,1'-biphenyl]-4,4'-diyl)diacetamide. Yield : ~ 4 g.

Step 2: Without further purification, 3 g of N, N'-(3,3',5,5'-tetramethyl-[1,1'-biphenyl]-4,4'-diyl)diacetamide is added into 50 mL H_2O at 90 °C, to which a solution containing 30 g of

$KMnO_4$ in 300 mL is added dropwise. The reaction mixture is further stirred for 36 hours at 100 °C. After cooling down to room temperature, the solution is filtered, and the filtrate is acidized with HCl to pH = 2~3, the precipitate is filtered, washed copiously with deionized water to give light yellow solid of 4,4'-diacetamido-[1,1'-biphenyl]-3,3',5,5'-tetracarboxylic acid. Yield : ~ 0.9 g.

Step 3: 1 g of 4,4'-diacetamido-[1,1'-biphenyl]-3,3',5,5'-tetracarboxylic acid is added into 100 mL H_2O containing 5 mL of concentrated HCl. The reaction mixture is further stirred for 12 h at 100 °C. After cooling down to room temperature, the solution is filtered, and washed copiously with deionized water, and dried at 70 °C to give 4,4'-diamino-[1,1'-biphenyl]-3,3',5,5'-tetracarboxylic acid. Yield : ~ 0.7 g. ^{1}H NMR (DMSO-*d6,* 400 MHz: δ (ppm) 8.18 (s, 4H, -C-H)); ^{13}C NMR (DMSO-*d6,* 100 MHz, δ (ppm) 169.11, 151.55, 133.89, 124.07, 112.47.

Synthesis of MOF.

The mixture containing 0.05 mmol NH_2-H_4BPTC, 0.1 mmol $NiCl_2 \cdot 6H_2O$, 3 mL DMF and 3 mL H_2O was sealed in a vessel (25 mL). The vessel was heated to 100 °C at a heating rate of 4 °C h^{-1} for 72 h, and then cooled to RT within 8 h to give pale-green crystals (yield: 80%, based on $NiCl_2$). Anal. Calcd for $C_8H_8NNiO_6$: C, 35.22; H, 2.96; N, 5.13%. Found: C, 35.45; H, 3.01; N, 5.34%.

X-ray crystallography.

A Bruker Smart Apex II CCD detector was used to collect the single crystal data at 150(2) K using Mo Kα radiation (λ = 0.71073 Å). The structure was solved by direct methods and refined by full-matrix least-squares refinement based on F^2 with the SHELXTL program. The non-hydrogen atoms were refined anisotropically with the hydrogen atoms added at their geometrically ideal positions and refined isotropically. As the disordered solvent DMF molecules in the structure cannot be located, the SQUEEZE routine of Platon program was applied in refining. The formula of complex was got by the single crystal analysis together with elemental microanalyses and TGA data. Relevant crystallographic results are listed in Table S4. Selected bond lengths and angles are provided in Table S5.

GCMC simulation.

Grand canonical Monte Carlo (GCMC) simulations were performed for the gas adsorption in the framework by the Sorption module of Material Studio (Accelrys. Materials Studio Getting Started, release 5.0). The framework was considered to be rigid, and the optimized gas and epoxide molecules were used. The partial charges for atoms of the framework were derived from Q_{Eq} method and Q_{Eq} neutral 1.0 parameter. The interaction energies between the gas molecules and framework were computed through the Coulomb and Lennard-Jones 6-12 (LJ) potentials. All parameters for the atoms were modeled with the universal force field (UFF) embedded in the MS modeling package. A cutoff distance of 12.5 Å was used for LJ interactions, and the Coulombic interactions were calculated by using Ewald summation. For each run, the 3×10^6 maximum loading steps, 3×10^6 production steps were employed.

Breakthrough experiments.

The breakthrough experiment was performed on the Quantachrome dynaSorb BT equipments at 298 K and 1 bar with an equal volume of mixed gas (gas A: gas B: Ar = 5% : 5% : 90%, Ar as the carrier gas, flow rate = 7 mL min^{-1}). The activated **1** (0.7 g) was filled into a packed column of ϕ 4.2×80 mm, and then the packed column was washed with Ar at a rate of 7 mL min^{-1} at 343 K for 60 minutes to further activate the samples. Between two breakthrough experiments, the adsorbent was regenerated by Ar flow of 7 mL min^{-1} for 35 min at 353 K to guarantee a complete removal of the adsorbed gases.

On the basis of the mass balance, the gas adsorption capacities can be determined as follows:

$$Q_i = \frac{C_i V}{22.4 \times m} \times \int_0^t (1 - \frac{F}{F_0}) dt$$

Where Q_i is the equilibrium adsorption capacity of gas i (mmol g^{-1}), C_i is the feed gas concentration, V is the volumetric feed flow rate (cm^3 min^{-1}), t is the adsorption time (min), F_0 and F are the inlet and outlet gas molar flow rates, respectively, and m is the mass of the adsorbent (g).

Calculation of sorption heat using Virial 2 mode.

$$In(P) = In(N) + \frac{1}{T}\sum_{i=0}^{m} a_i N^i + \sum_{j=0}^{n} b_j N^j \qquad Q_{st} = -R\sum_{i=0}^{m} a_i N^i$$

The above expression was used to fit the combined isotherm data for **1** at 273 and 298 K, where P is the pressure, N is the adsorbed amount, T is the temperature, a_i and b_j are virial coefficients, and m and N are the number of coefficients used to describe the isotherms. Q_{st} is the heat of adsorption and R is the universal gas constant.

IAST adsorption selectivity calculation.

The experimental isotherm data for pure C_2H_2, CO_2 and CH_4 (measured at 298K) was fitted using a single-site Langmuir-Freundlich (L-F) model:

$$q = a_1 \frac{a_1 * b_1 * P^{c_1}}{1 + b_1 * P^{c_1}}$$

Where q and p are the adsorbed amounts and the pressure of component i, respectively.

The adsorption selectivity for binary mixtures defined by

$$S_{i/j} = \left(\frac{x_i * y_j}{x_j / y_i}\right)$$

was calculated using the Ideal Adsorption Solution Theory (IAST) of Myers and Prausnitz. Where xi is the mole fraction of component i in the adsorbed phase and yi is the mole fraction of component i in the bulk.

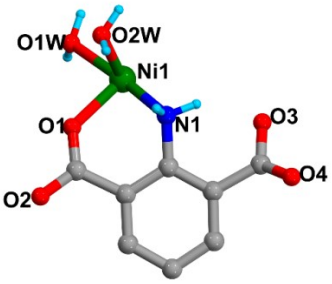

Figure S1. The asymmetric unit of **1**.

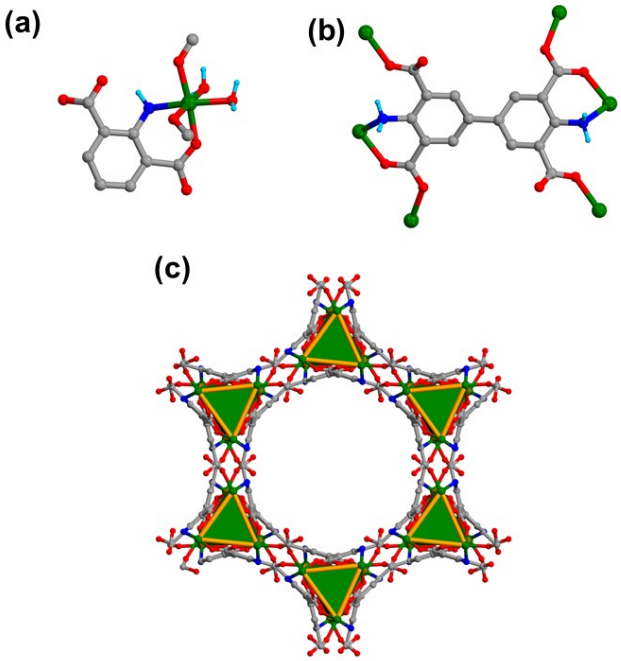

Figure S2. (a) Coordination environment of Ni^{2+} ions; (b) coordination mode of NH_2-$BPTC^{4-}$; (c) view of the 1D channel.

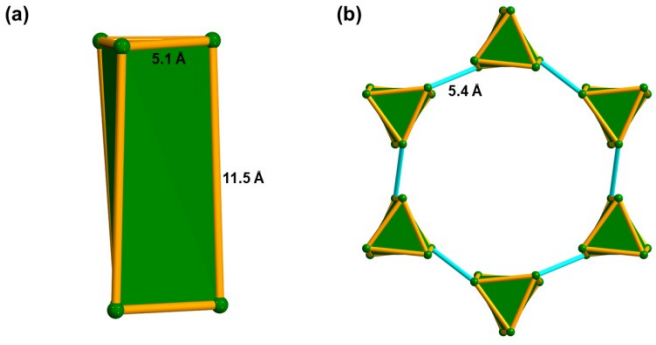

Figure S3. (a) SBU-SBU distance (Ni1···Ni1) and cross-section triangle size in a SBB; (b) separation distance in adjacent SBBs.

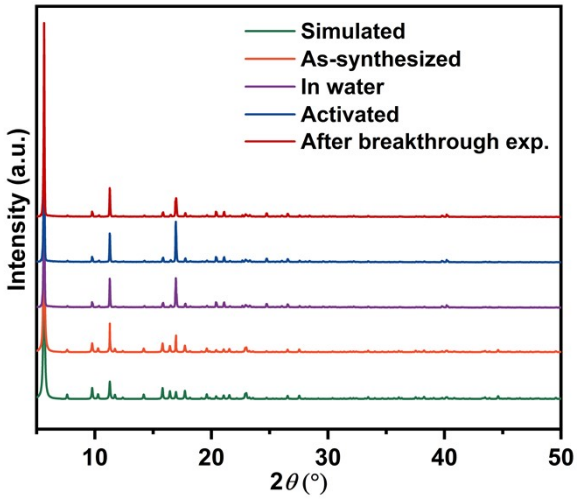

Figure S4. PXRD patterns of **1** obtained by different treated methods.

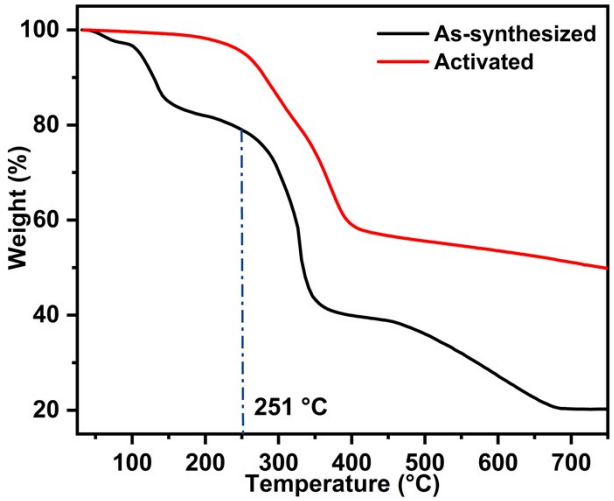

Figure S5. TGA curve for **1**.

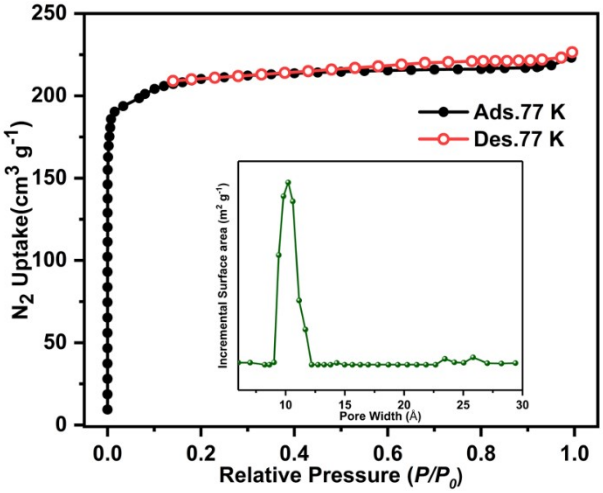

Figure S6. Sorption isotherm of N_2 at 77 K and PSD curve using NLDFT mode.

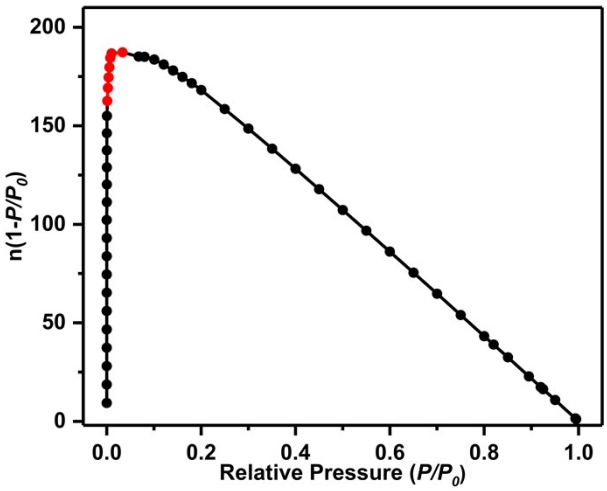

Figure S7. The consistency plot.

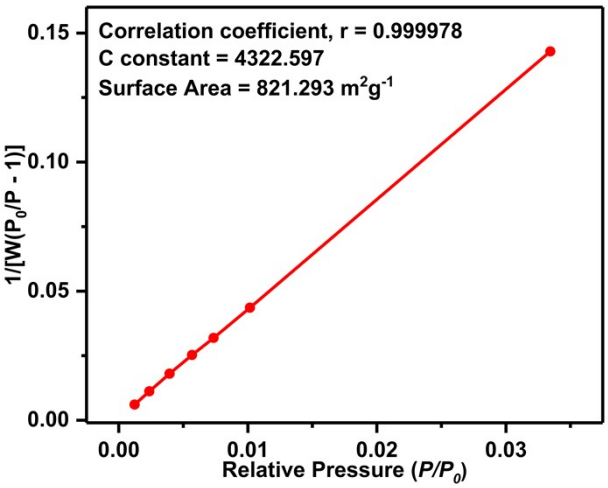

Figure S8. BET surface area plot.

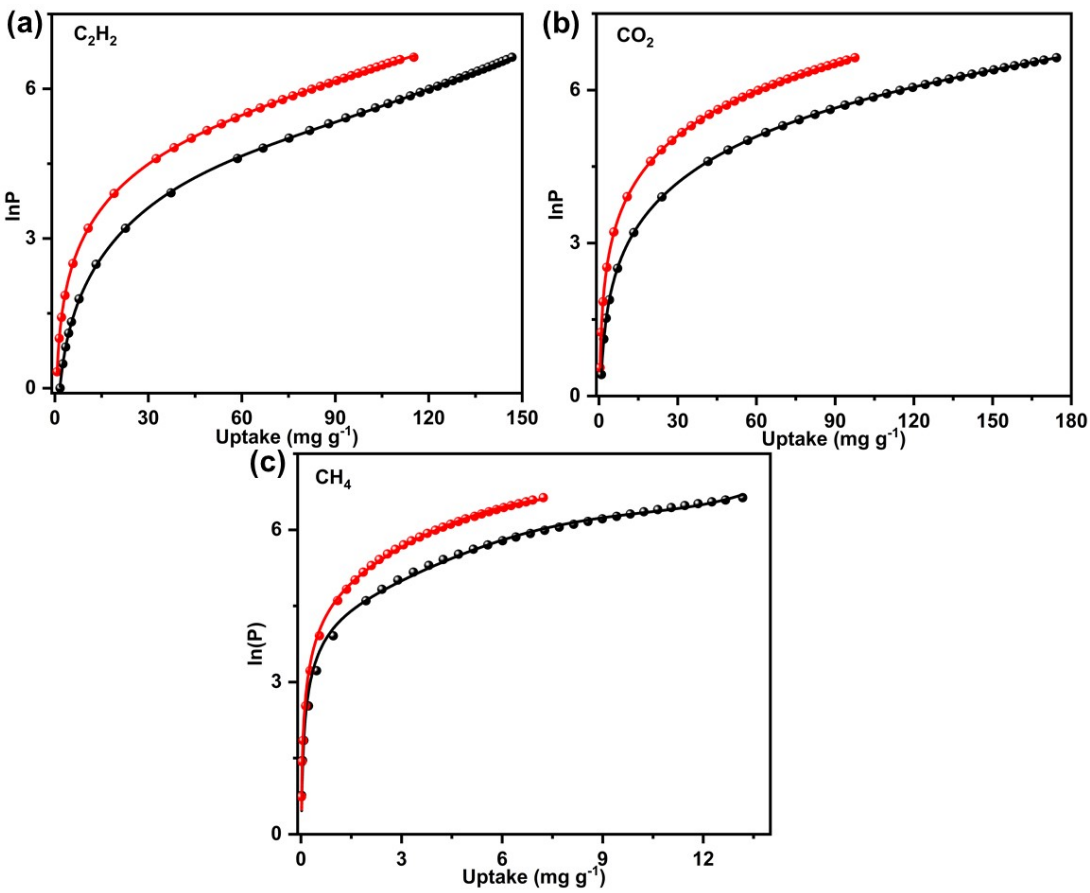

Figure S9. Fitted isotherms of **1** measured at 273 and 298 K.

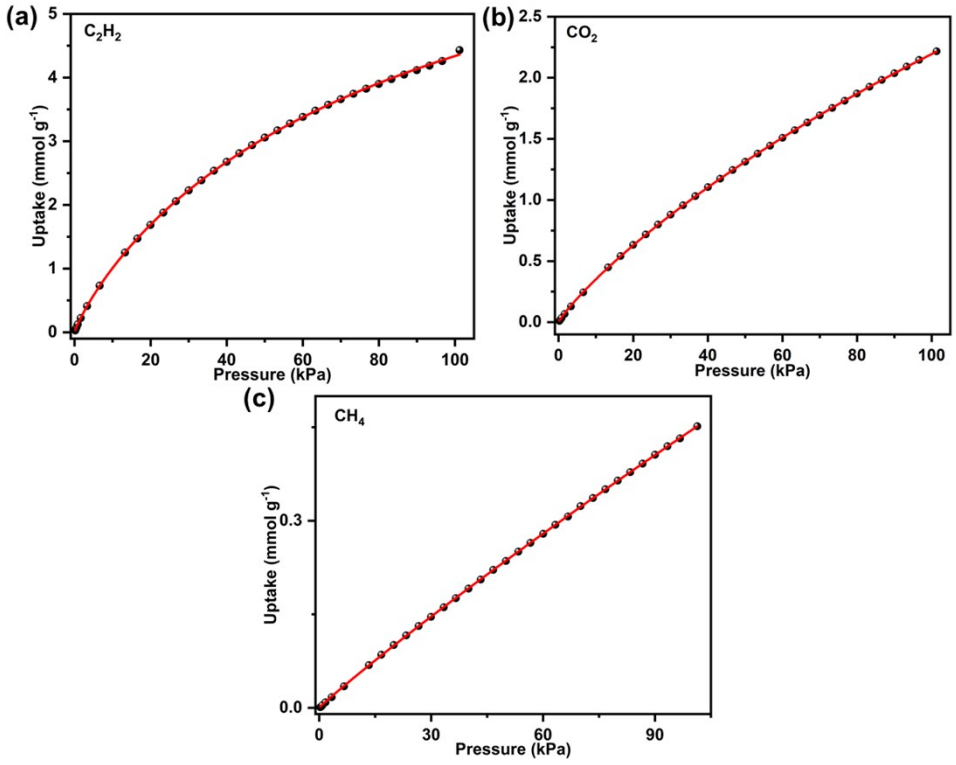

Figure S10. (a-c) Gas adsorption isotherms of **1** fitted by L-F model.

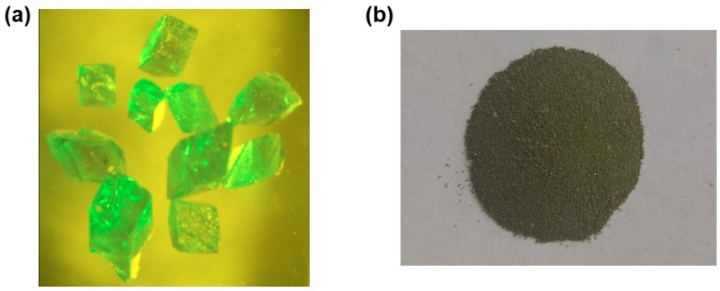

Figure S11. (a) Photograph of the crystal; (b) activated sample.

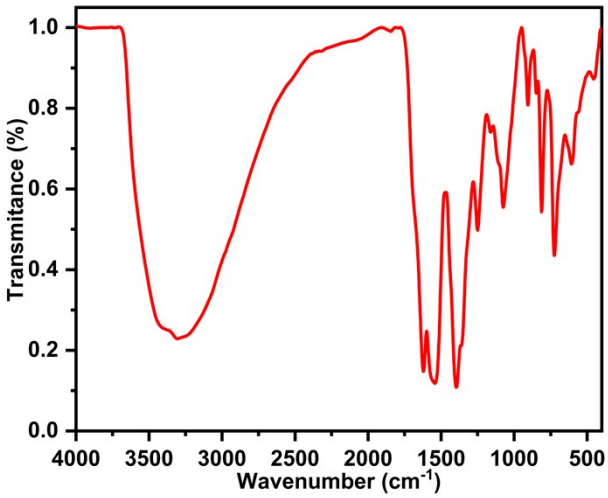

Figure S12. FTIR spectra of the as-synthesized sample of **1**.

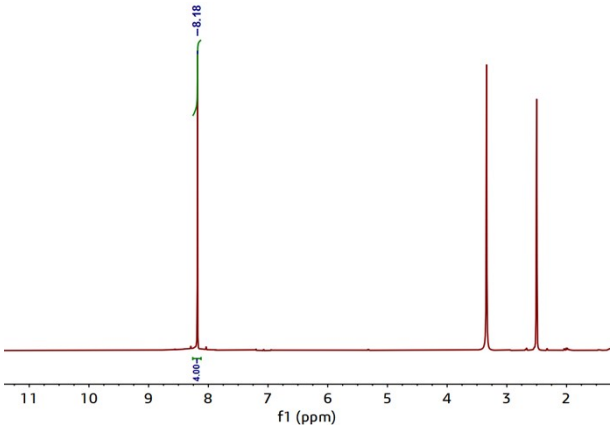

Figure S13. ^{1}H-NMR spectrum of NH_2-H_4BPTC.

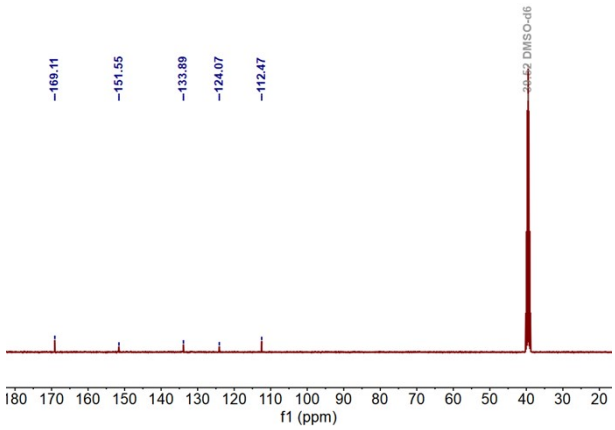

Figure S14. ^{13}C NMR spectrum of NH_2-H_4BPTC ligand.

Table S1. Comparison of state-of-the-art materials for C_2H_2 uptake at 1 bar.

Adsorbent	C_2H_2 (cm^3/g)	C_2H_2 (cm^3/cm^3)	References
CPM-733-dps	234	204	S1
FJI-H8	224	196	S2
CoMOF-74	191	230	S3
Mg-MOF-74	187.5	167	S3
Cu-TDPAT	177.7	148.6	S4
BUT-11	159.9	144.7	S5
NOTT-300	142	147.6	S6
UPC-200(Fe)-F-BIM	139.8	100.8	S7
[Zn_2(DHTP)]	122	150	S8
Tm_2(OH-bdc)$_2$(μ_3-OH)$_2$	118	140	S9
UTSA-74	107.5	144.1	S10
1	99.3	110.5	This work
MECS-5	86.2	118.0	S11
HUST-6	78.3	60.2	S12
JNU-1	60.0	89.8	S13
JXNU-5a	55.9	72.6	S14
BSF-2	42	52	S15
SNNU-150-In	35.0	24.5	S16

Table S2. Comparison of quadrupolar moment of C_2H_2, CO_2 and CH_4.

Adsorbate	Quadrupolar moment ($\times 10^{-26}$ esu cm^2)
C_2H_2	7.2
CO_2	4.3
CH_4	0

Table S3. Comparison of MOF materials for C_2H_2-CO_2 at 1 bar and 298 K.

Adsorbent	S_{AC} (C_2H_2-CO_2)	References
NKMOF-1-Ni	30	S17
$Ni_3(COOH)_6$	22	S18
TCuCl	16.9	S19
Pacs-CoMOF-2a	13	S20
TiFSIX-2-Cu-i	6.5	S21
SIFSIX-Cu-TPA	5.3	S22
Cu-CPAH	3.6	S23
1	**3.5**	**This work**
Cu-tztp MOF 1a	2.7	S24
Zn-MOF-74	2	S10
SNNU-17	1.2	S25

Table S4. Crystal Data and Structure Refinements for MOF **1**.

Empirical formula	$C_8H_8NNiO_6$
Formula weight	272.86
Temperature/K	296(2)
Crystal system	Trigonal
Space group	*P*-31*c*

a/Å	18.104(4)
b/Å	18.104(4)
c/Å	17.218(4)
α/°	90
β/°	90
γ/°	120
Volume/Å^3	4887(3)
Z	12
ρ_{calc}g/cm^3	1.113
F(000)	1668
Crystal size/mm^3	0.14 × 0.13 × 0.10
Radiation	Mo K_α (λ = 0.71073)
Reflections collected	24347
R_{int}	R_{int}= 0.1148
Goodness-of-fit on F^2	0.927
R_1, wR_2 [I > 2σ(I)]	R_1= 0.0450, wR_2= 0.0972
R_1, wR_2 [all data]	R_1= 0.0830, wR_2= 0.1107

$$R_1 = \sum \left| |F_0| - |F_c| \right| / \sum |F_0| \qquad wR_2 = \left[\sum \left[w(F_0^2 - F_c^2) \right] / \sum \left[w(F_0^2)^2 \right] \right]^{1/2}$$

Table S5. Selected bond lengths [Å] and angles [°] for MOF **1**.

Ni(1)-O(3)#1	2.026(2)	O(3)#1-Ni(1)-O(1)	172.75(9)
Ni(1)-O(1)	2.033(2)	O(3)#1-Ni(1)-N(1)	90.21(9)
Ni(1)-N(1)	2.066(2)	O(1)-Ni(1)-N(1)	83.06(9)
Ni(1)-O(2)#2	2.068(2)	O(3)#1-Ni(1)-O(2)#2	91.52(9)
Ni(1)-O(1W)	2.083(2)	O(1)-Ni(1)-O(2)#2	91.29(8)

Ni(1)-O(2W)	2.100(2)	N(1)-Ni(1)-O(2)#2	90.95(9)
O(1)-C(8)	1.268(3)	O(3)#1-Ni(1)-O(1W)	95.47(9)
O(2)-C(8)	1.260(3)	O(1)-Ni(1)-O(1W)	90.98(9)
O(2)-Ni(1)#3	2.068(2)	N(1)-Ni(1)-O(1W)	172.14(9)
O(3)-C(1)	1.201(4)	O(2)#2-Ni(1)-O(1W)	94.31(8)
O(3)-Ni(1)#1	2.026(2)	O(3)#1-Ni(1)-O(2W)	90.24(9)
O(4)-C(1)	1.416(6)	O(1)-Ni(1)-O(2W)	86.73(9)
O(4A)-C(1)	1.405(6)	N(1)-Ni(1)-O(2W)	87.07(10)
O(4A)-O(4A)#4	1.425(10)	O(2)#2-Ni(1)-O(2W)	177.36(9)
O(1W)-H(1WA)	0.85	O(1W)-Ni(1)-O(2W)	87.48(9)

Symmetry codes: #1 -x+2, -y+1, -z+1, #2 -y+1, x-y, z, #3 -x+y+1, -x+1, z, #4 x, x-y, -z+1/2.

Table S6. Fitting results by Virial 2 model.

	a_0	a_1	a_2	b_0	b_1	Chi^2	R^2
C_2H_2	-3863.505	56.130	-0.841	13.581	-0.166	0.01485	0.99995
CO_2	-3006.927	-3.192	0.138	11.481	0.024	0.00070	0.99999
CH_4	-1040.420	-637.046	10.378	8.192	1.942	0.47560	0.99703

Table S7. Fitting results by L-F model.

	a_1	b_1	c_1	Chi^2	R^2
C_2H_2	8.713	0.0017	0.880	0.00703	0.99990
CO_2	10.997	0.0044	0.878	0.00028	0.99998
CH_4	8.740	0.0007	0.956	0.00002	0.99998

References

1. Y. Wang, X.-X. Jia, H.-J. Yang, Y.-X. Wang, X.-T. Chen, A.-N. Hong, J.-P. Li, X.-H. Bu, and P.-Y. Feng, *Angew. Chem., Int. Ed*., 2020, **59**, 19027-19030.
2. J. Pang, F. Jiang, M. Wu, C. Liu, K. Su, W. Lu, D. Yuan, M. Hong, *Nat. Commun*. 2015, **6**, 7575.
3. S. Xiang, W. Zhou, Z. Zhang, M. A. Green, Y. Liu, B. Chen, *Angew. Chem., Int. Ed*.,

2010, **49**, 4615-4618.

4. K. Liu, D. Ma, B. Li, Y. Li, K. Yao, Z. Zhang, Y. Han, Z. Shi, *J. Mater. Chem. A*, 2014, **2**, 15823-15828.
5. X.-Q. Wang, L.-B. Li, Y Wang, J.-R. Li and J.-P. Li, *CrystEngComm*, 2017, **19**, 1729-1737.
6. S.-H Yang, A.-J. Ramirez-Cuesta, R. Newby, V. Garcia-Sakai, P. Manuel, S.-K. Callear, S.-I. Campbell, C.-C. Tang and M. Schröder, *Nature Chem*., 2015, **7,** 121-129.
7. W. Fan, S. Yuan, W. Wang, L. Feng, X. Liu, X. Zhang, X. Wang, Z. Kang, F. Dai, D. Yuan, D. Sun, H.-C. Zhou, *J. Am. Chem. Soc.,* 2020, **142**, 8728-8737.
8. J. Pang, F. Jiang, M. Wu, C. Liu, K. Su, W. Lu, D. Yuan, M. Hong, *Nat. Commun*., 2015, **6**, 7575.
9. D. Ma, Z. Li, J. Zhu, Y. Zhou, L. Chen, X. Mai, M. Liu, Y. Wu, Y. Li, *J. Mater. Chem. A*, 2020, **8**, 11933-11937.
10. F. Luo, C. Yan, L. Dang, R. Krishna, W. Zhou, H. Wu, X. Dong, Y. Han, T. L. Hu, M. O'Keeffe, L. Wang, M. Luo, R. B. Lin and B. Chen, *J Am Chem Soc*, 2016, **138**, 5678-5684.
11. X.-J. Hong, Q. Wei, Y.-P. Cai, B.-B. Wu, H.-X. Feng, Y. Yu and R.-F. Dong, *ACS Appl Mater Interfaces*, 2017, **9**, 29374-29379.
12. F. Yu, B. -Q. Hu, X. -N. Wang, Y. -M. Zhao, J. -L. Li, B. Li and H. -C. Zhou, *J. Mater. Chem. A*, 2020, **8**, 2083-2089.
13. H. Zeng, M. Xie, Y.-L. Huang, Y. Zhao, X.-J. Xie, J.-P. Bai, M.-Y. Wan, R. Krishna, W. Lu and D. Li, *Angew. Chem., Int. Ed*., 2019, **58**, 8515-8519.
14. R. Liu, Q.-Y. Liu, R. Krishna, W.-J. Wang, C.-T. He and Y.-L. Wang, *Inorg. Chem*., 2019, **58**, 5089-5095.
15. Y. Zhang, L. Yang, L. Wang, X. Cui and H. Xing, *J. Mater. Chem*. *A*, 2019, **7**, 27560-27566.
16. H.-J. Lv, Y.-P. Li, Y.-Y. Xue, Y.-C. Jiang, S.-N. Li, M.-C. Hu and Q.-G. Zhai, *Inorg Chem*, 2020, **59**, 4825-4834.
17. Y.-L. Peng, T. Pham, P.-F. Li, T. Wang, Y. Chen, K.-J. Chen, K.-A. Forrest, B. Space, P. Cheng, M.-J. Zaworotko and Z.-J. Zhang, *Angew. Chem. Int. Ed*., 2018, **57**, 10971-10975.

18. L. Zhang, K. Jiang, J. Zhang, J.-Y. Pei, K. Shao, Y.-J. Cui, Y. Yang, B. Li, B.-L Chen and G.-D. Qian, *ACS Sustainable Chem. Eng*., 2019, **7**, 1667-1672.
19. S. Mukherjee, Y. He, D. Franz, S.-Q. Wang, W.-R. Xian, A.-A. Bezrukov, B. Space, Z. Xu, J. He, J.-M. Zaworotko, *Chem. Eur. J*., 2020, **26**, 4923-4929.
20. D.-M. Chen, C.-X. Sun, N.-N. Zhang, H.-H. Si, C.-S. Liu, and M. Du, *Inorg. Chem*., 2018, **57**, 2883-2889.
21. K.-J. Chen, H.-S. Scott, D.-G. Madden, T. Pham, A. Kumar, A. Bajpai, M. Lusi, K.-A. Forrest, B. Space, J.-J. Perry and M.-J. Zaworotko, *Chem*, 2016, **1**, 753-765.
22. H. Li, C.-P Liu, C. Chen, Z.-Y Di, D.-Q. Yuan, J.-D Pang, W. Wei, M.-Y Wu and M.-C Hong, *Angew. Chem. Int. Ed*., 2021, **60**, 7547-7552.
23. L.-K Meng, L.-X. Yang, C.-L Chen, X.-L. Dong, S.-Y. Ren, G.-H. Li, Y. Li, Y. Han, Z. Shi, and S.-H. Feng, *ACS Appl. Mater. Interfaces*, 2020, **12**, 5999-6006.
24. X.-Y. Li, Y.-Z. Li, L.-N. Ma, L. Hou, C.-Z. He, Y.-Y. Wang and Z. Zhu, *J. Mater. Chem. A*, 2020, **8**, 5227-5233.
25. H.-P. Li, Y.-Y. Xue, Y. Wang, H. Sun, M.-C. Hu, S.-N. Li, Y. Jiang, Q.-G. Zhai, *Cryst. Growth Des*. 2021, **21**, 1718-1726.